Automated determination of wave run up from time-variance video images

by

Sebastian J. Pitman

This thesis is submitted to Plymouth University
in partial fulfilment of the requirements for the degree of

MRes Applied Marine Science

Plymouth University
Faculty of Science and Environment

School of Marine Science and Engineering,
Plymouth University, Devon. PL4 8AA

September 2013

This thesis is submitted in the format of
The Journal of Coastal Research

Automated determination of wave run up from time-variance video images

Sebastian J. Pitman[†]

[†]**School of Marine Science and Engineering,**
Plymouth University,
Devon.
UNITED KINGDOM
PL4 8AA
sebastian.pitman@postgrad.plymouth.ac.uk

ABSTRACT

A novel remote sensing method is presented that accurately predicts 2% run up and run down thresholds on a gravel beach under calm (H_s < 2 m) conditions. This overcomes the common problem of ascertaining accurate field measurements in the energetic swash zone of a gravel beach where damage to equipment is commonplace. The optical image intensity from time-exposure and time-variance Argus images is interrogated in order to extract the swash parameters of interest. Predictions are validated against field observation and result in a vertical RMS error of 17 cm for run up and 18 cm for back wash. The method alleviates the need for manual digitisation of swash events as has previously been commonplace, enabling swift creation of large datasets for validation of empirical formulae. The use of time-variance images was also seen to increase the number of useable images collected from Argus stations in adverse conditions when compared to time-exposure imagery. This paper outlines a solid proof of concept for the method but acknowledges that extensive further field validation is required, specifically under energetic conditions and at other gravel beaches.

ADDITIONAL INDEX WORDS: *Run up, time-variance, Argus, gravel beach, image-processing, backwash.*

INTRODUCTION

The beachface is a hugely dynamic zone in both a spatial and temporal sense, predominantly a result of swash processes such as run up. The foreshore of the beach (the intermittently wetted, intertidal area) acts as the interface zone between land and sea and is characterised by highly variable hydro- and morphodynamic processes. Understanding the evolution of the foreshore is of critical importance to coastal oceanographers, planners and engineers as much of the energy delivered to this region feeds into the erosive or accretive response of the beach (Stockdon *et al.,* 2006). Swash action is the dominant process responsible for moving sediment cross-shore between the subaerial and subaqueous zones, with a significant part of the littoral drift also taking place in this zone (Masselink and Puleo, 2006). The swash zone itself is defined as the boundary between the inner surf zone and the back beach (Ruggiero, Holman, and Beach, 2004) and its dominant responses are largely well understood. It is the most energetic zone in terms of bed sediment movement, typically characterised by strong and unsteady flows as a result of run up and backwash, within which single events can cause changes of up to 43 mm in bed level (Blenkinsopp *et al.,* 2011). It is important to recognise that this swash zone is part of an integrated system comprising local groundwater dynamics, the beachface and the surf zone, with the feedback from surf to swash of critical importance (Masselink and Puleo, 2006). It has also recently been shown that swash zone flows exert influence not just locally (overtopping, littoral drift, etc.), but they also affect the dynamics of the surf zone itself (Brocchini, 2006).

Run up is described here as a set of discrete water level maxima measured on the foreshore with respect to the still water level; that which would occur in the absence of forcing by the incident wave field (Stockdon *et al.,* 2006). This excursion up the beach is typically defined in terms of its vertical elevation, rather than the horizontal extent of run up (Holland *et al.,* 1995). The two components of run up; wave swash and wave set-up, operate on very different scales, as a result of the different forcing factors (Senechal *et al.,* 2011). Swash, the time-varying, fluctuating component, operates on frequencies comparable to the incident wave field from which it stems whereas set-up refers to the mean water level as a result of wave breaking (Komar, 1998; Senechal *et al.,* 2011). The wave run up height is generally normalised by the

incident wave height, as they are of the same order of magnitude (Kobayashi, 1997). Set-up is relatively small when compared to swash action on a steeply sloping beach, where there is an appreciable degree of wave reflection (Battjes, 1974). This wave driven run up converts kinetic energy into potential energy as it traverses up the beachface (up-rush phase), before gravity driven flows act to return the flow down the slope of the foreshore (backwash phase). There is typically interference between subsequent waves, with the backwash of preceding waves colliding with the uprush of the next wave, meaning individual waves do not often complete a full and balanced cycle of uprush and backwash (Erikson, Larson, and Hanson, 2005).

When determining various morpho- and hydrodynamic properties and states of the beach, it is common to turn to the non-dimensional Irribarren number or surf similarity parameter (Battjes, 1974),

$$\xi = \frac{\beta}{(H_o/L_o)^{1/2}} \quad (1)$$

where β is beach slope, L_o is the deepwater wavelength given by linear theory and H_o is the offshore wave height. This is often referred to as a dynamic beach steepness parameter (Stockdon *et al.,* 2006), accounting for the antecedent beach slope as well as the incident wave conditions. This property has proved useful in empirically determining run up (Holman, 1986; Holman and Sallenger, 1985; Ruggiero, Holman, and Beach, 2004; Stockdon *et al.,* 2006) and illustrates well the dependence of run up on beach slope and wave conditions.

Predictive formulas for run up are critical for coastal planners, engineers and researchers, because they provide estimation based on relatively easy to measure variables such as the offshore wave conditions and beach slope. Conversely, the in-situ measurement of swash processes are inherently difficult and complex (Blenkinsopp *et al.,* 2011), proving challenging for even the most robust and advanced hydrodynamic equipment (Masselink and Puleo, 2006). Many coastal processes, especially in the energetic swash zone, are poorly understood because of this difficulty in collecting continuous, long-term and large scale field measurements, especially with high spatial

and temporal resolution (Guedes *et al.,* 2011, Holman and Stanley, 2007). It is widely understood that the beach is constantly changing, especially under energetic conditions, which is when in-situ measurements would perhaps be of most use but least feasible. The dynamic nature of the beachface results in progressive negative feedback loops under energetic conditions, and the evolution of these loops acts to hamper swash action and ultimately protect the beach. These feedback loops are small in scale but important in nature and are often missed when field experiments are reduced to conducting only pre- and post-event profiling because conditions during the event were too energetic (Matias *et al.,* 2012). This is a limitation that is further amplified when considering research on gravel beaches, where delicate and expensive instruments are typically exposed to, and damaged by, large pieces of sediment being transported in the water column, hampering the acquisition of meaningful measurement (Masselink *et al.,* 2010). The recent work of Poate *et al.,* (2013) represents some of the first comprehensive high-frequency, high resolution research on a gravel beach exposed to energetic wave conditions, achieved through the combination of in-situ measurement and remote sensing. The conclusion of their research was that given the potential for damage to in-situ equipment, future work under energetic waves may be confined to remote image analysis and low tide surveys.

Remote sensing systems that are able to monitor coastal processes, such as the Argus video imaging system, have enjoyed a period of significant interest and development over the past 30 years (Guedes *et al.,* 2011; Holman and Stanley, 2007). Progress in this area is driven, in no minor part, by the aforementioned difficulties in obtaining in-situ measurement. Argus systems typically comprise a cluster of up to 5 cameras positioned overlooking the coastal area of interest, capturing images at regular time intervals and uploading them to a computer-based archive and control system (Holman and Stanley, 2007).

Argus stations typically sample once or twice every hour, producing three outputs; snapshot, time exposure and time variance images (Figure 1). Snapshot (snap) images are rarely used for quantitative analysis, but give a good qualitative overview of the study area (Holman and Stanley, 2007). Time exposure (timex) images have become the most popular Argus output, generally collected hourly, representing the

Figure 1. Example snap (top), timex (middle) and variance (bottom) images obtained from camera 1 at Slapton Sands during energetic conditions on 17 June 2013. The dynamic range on the variance image has been enhanced for ease of viewing.

mathematical time-mean of all frames over a sample period (typically ~600 images collected at 1 Hz), which generally represents a 10 min time frame (Guedes *et al.,* 2011). These images are useful in giving an overview of persistent processes, averaging out moving components such as breaking waves into a distinct white band. Time variance (variance) images are perhaps the least used image type and are comprised of the variance in image intensities over the sample period, or otherwise, the standard

deviation in pixel intensity over the sample period. These images are characterised by bright areas representing high variability in pixel intensity over time (such as the surf and swash zones), whereas dark areas represent low variability in intensities (such as subaerial beach or the region seaward of the surf zone). Quantitative data is obtained by interrogating the image for optical signatures that are either directly or indirectly created by nearshore processes, such as the concentration of breaking waves over a submerged bar showing up as a high intensity band in the image (Kingston *et al.,* 2000; Lippmann and Holman, 1989, 1990; Plant and Holman, 1998). The Argus system has also proved useful in remotely sensing wave period (Stockdon and Holman, 2000), wave incidence angle (Herbers and Guza, 1990) and shoreline (Aarninkhof *et al.,* 2003), among other parameters.

In terms of run up, remote sensing methods have often produced results comparable to those obtained in the field by direct measurement methods such as resistance wires (Holland *et al.,* 1995). Indeed, image analysis can provide a better estimation as it provides a bed-level reading, whereas the accuracy of other instrumentation is typically a function of its height above the bed, although it is acknowledged that laser scanning and other bed-level sensory methods do exist (e.g., Almeida *et al.,* 2013). The most widely used method of remotely sensing run up involves decomposing timex images into their individual frames and digitising the position of the water-level frame by frame (Aagaard and Holm, 1989; Holman and Guza, 1984). This method was typically done manually with times of 30 minutes reported for the digitisation of a 2048 point (34 minute) dataset (Holman and Guza, 1984). Semi-automated algorithms have been developed which reduce the processing time; however, some researchers still favour manual digitisation for accuracy (Senechal *et al.,* 2011). The digitisation of run up typically produce observations of swash height that have a standard deviation on measured swash height of around 5-10% when compared with field measurement using methods such as resistance wires.

The weather proves to be a significant limiting factor when relying on the use of video images to remotely sense the beachface. The cameras are highly susceptible to fog and low light which hamper their ability to collect data, although enhanced cameras and those that work using infra-red are available but very expensive (Holman and Stanley,

2007). They are further affected by rain which can get onto the lens covers and sunlight, which at low incidence angles provides too much reflection to make the images of any quantitative use. Furthermore, in order to extract run up data, topographic data is required for the area of interest in the image (Almeida *et al.,* 2013). Despite these limitations, the enhanced spatial and temporal coverage offered by coastal video systems and their low susceptibility to storm damage makes them attractive and hugely beneficial to researchers. Argus systems can typically be in place for many years, constantly recording with very little maintenance, meaning they capture all manner of events that can later be analysed; a typical system logging 1 image per hour over 14 hours of daylight can produce over 5000 discrete observations per year for analysis. A significant drawback of existing methods to quantify run up is the need to manually digitise all the component images, whereas a method that only requires the processing of one time lapse image (the time mean of all component images) would be hugely beneficial. This research will take the images as a whole, rather than deconstructing them into the composite frames as has been common practice in prior studies. This is of particular interest to those whom wish to improve empirical parameterisations of run up but whom lack sufficient field data with which to validate formulae as data can be generated far quicker when the need to digitise is removed.

The use of video imaging to detect the shoreline position has typically resulted in errors comparable in magnitude to the width of the swash zone, as a result of the dynamic nature of the line that these methods try to pick out. Guedes *et al.,* (2001) showed the area of highest intensity not to be over submerged bars, but instead to be coincident with the swash zone, as a result of the wetting and drying producing high variance.

The aim of this work is to investigate the optical signature of the swash zone in variance and timex images, in an attempt to extract the run up and backwash limits of the swash. This has the obvious benefit of removing the need for time consuming digitisation of run up events on a frame by frame basis, meaning much more run up data can be obtained by researchers in a time-effective way, for validation of empirical formulae. It perhaps seems counter-intuitive to examine processes that happen on

timescales of just a few seconds with methods that produce outputs sampled over a few minutes, but the very nature of the time-mean intensity should provide a good overview of the swash processes within this window. This paper presents a novel remote sensing method that ascertains the 2% run up exceedance (R_2) and the 2% backwash exceedance (D_2) thresholds from the complete images, validated against field observations on a gravel beach. This method allows for creation of a significant dataset that is subsequently compared against an established run up parameter.

METHODS

Study Area

Slapton Sands is a 4.5 km long, 100-140 m wide gravel barrier (D_{50} 2-10 mm) aligned roughly north-south in Start Bay with a typical beach gradient of 0.12. The barrier usually exhibits crest elevations of ≈5.5 m above Ordnance Datum Newlyn (ODN) at Torcross, rising to 8 m ODN at the northern end (Hails, 1975). The barrier fronts a fragile freshwater lagoon (Slapton Ley), which is currently at risk from Slapton's potential response to sea level rise; namely overtopping and overwash. The presence of the lagoon drives a seaward directed groundwater gradient across the breadth of the barrier (Austin and Masselink, 2006).

The tidal regime is predominantly macrotidal and bimodal (Figure 2) with spring and neap tide ranges of 4.3 and 1.5 m respectively, with average wave conditions characterised by H_s of 0.7 m, which increases to 2 - 4 m during storms. Southerly swell waves propagate up from the Atlantic but the barrier is largely protected from these by Start Point, a prominent headland that marks the southerly point of Start Bay, located 4 km south of Slapton Sands. However, some swell waves are able to refract towards the beach over Skerries Bank; a sub-surface bank of shelly sands (Hails, 1975). Easterly wind waves are the second modal wave condition and represent the most energetic wave conditions to affect the beach. The barrier is subject to c.15 storms per year, split between both easterly and southerly prevailing conditions. Southerly storms are seen to cause accretion in the supratidal zones and erosion in the intertidal zones, with an overall significant net loss in beach volume. Easterly storms induce supratidal erosion and intertidal accretion, resulting in significant net gain in overall beach

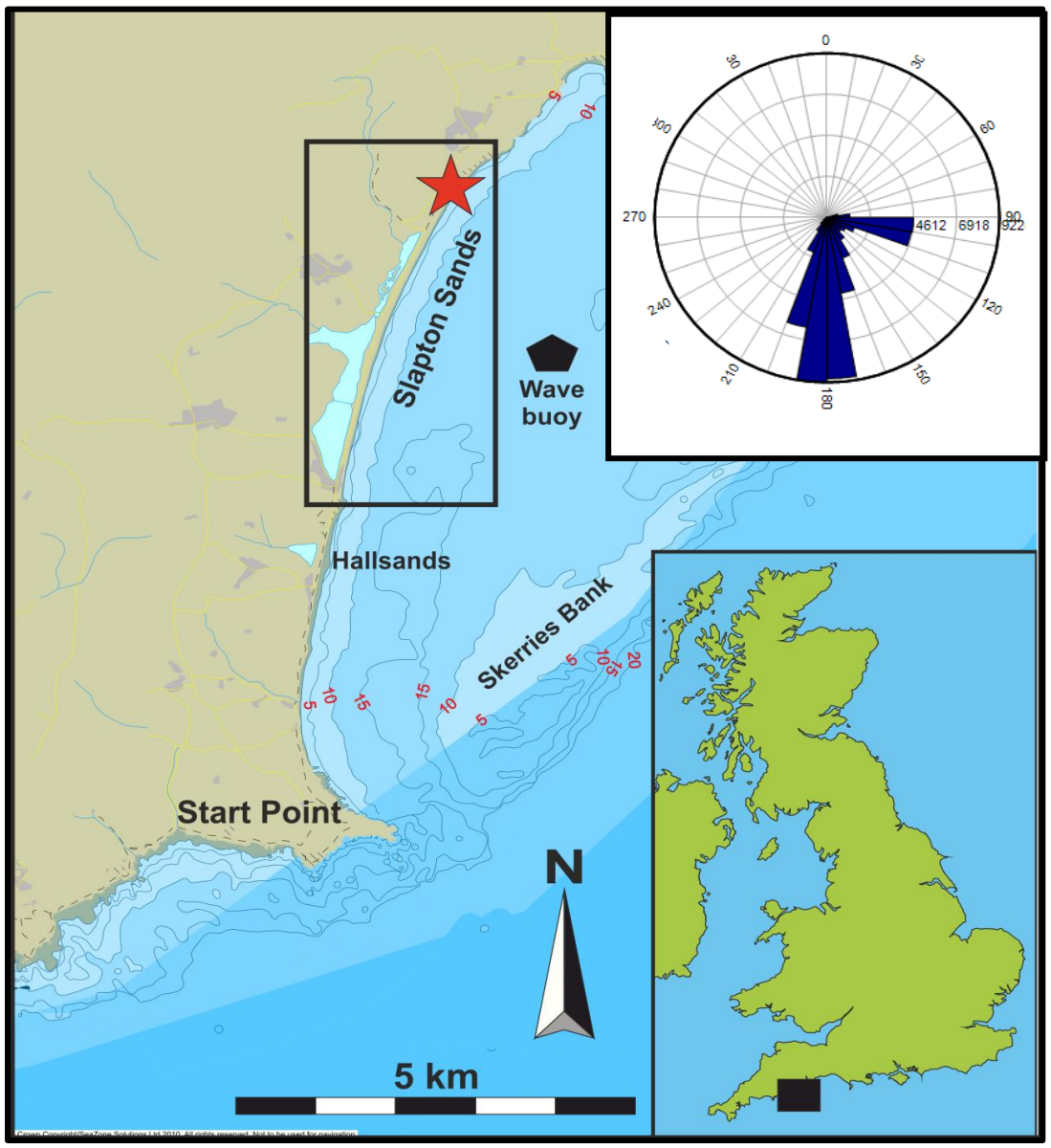

Figure 2. The location of Slapton Sands, including the position of the Argus station (red star) and wave buoy (black pentagon). The directional wave plot depicts all waves to reach Slapton during 2011.

volume (Ruiz de Alegria-Arzaburu and Masselink, 2010). A prominent step feature results in a distinct shore break and offshore slopes mean that a surf zone is rarely observed, apart from in the most energetic of conditions (H_s > 3 m).

Field Measurement

Field measurements were undertaken over a six week period between June and August 2013. The survey period was characterised by southerly swell, with H_s ranging from 0.2 m - 1.3 m, with survey days capturing both spring and neap tides (Figure 3). Wave conditions were obtained by a direction wave buoy moored in c.10 m water depth in Start Bay.

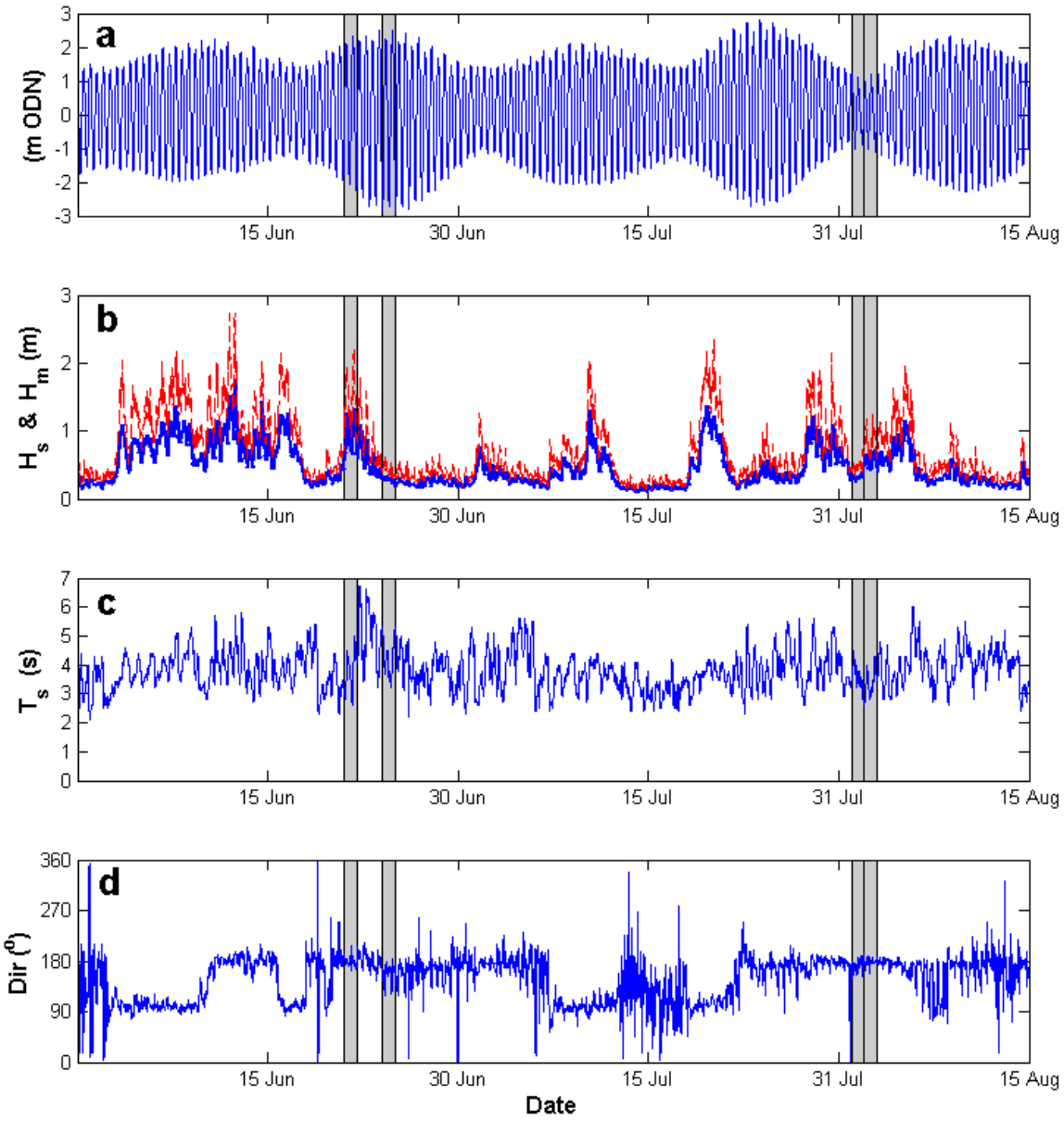

Figure 3. Time series of hydrodynamics for Slapton Sands during the study period in 2013. Tidal data (a) observed at Devonport and corrected using approved Admiralty corrections for Start Point; Significant wave height H_s (solid line) and maximum wave height H_m (dashed line) (b); Significant wave period T_s (c) and wave direction (d). Wave data were recorded by a waverider buoy within Start Bay. Grey rectangles represent the two survey days during which field measurement took place.

A cross-shore transect of fibreglass rods (1.2 m long and 8 mm diameter) was installed across the intertidal zone at 1-m intervals (Figure 4). The rod array was used to measure wave run up and run down over 10-min periods, coinciding with the capture time of the Argus cameras. These measurements were made around both low and high tides, and were estimated to the nearest 0.1 m in the horizontal plane. Run up was defined as the maximum propagation cross-shore of each event, with run down

defined as the final gravity-driven downslope water motion after the maximum extent of run up has been reached, when all flows are downslope and seawards (Foote and Horn, 1999). Run down was often interfered with by the subsequent swash event, and in this situation the lowest horizontal position that experienced gravity-driven seaward flow was taken. The rapidity of these swash events necessitated measurements being orally recorded and subsequently transcribed from recordings. R_2 was defined as the elevation that is exceeded by only 2% of swash events, and likewise D_2 was the elevation below which only 2% of the back wash events would pass. This was calculated for each discrete sample period from the cumulative frequency distribution of all the events in that period as per Figure 5.

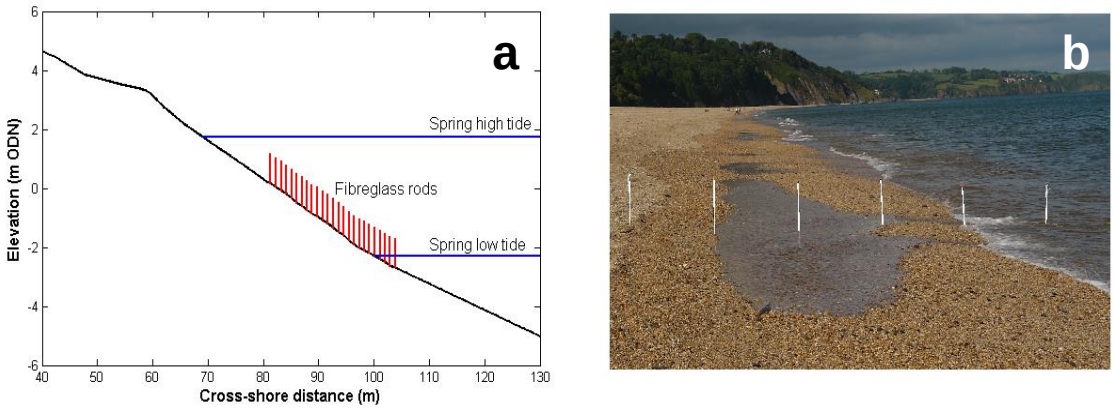

Figure 4. Schematic of experimental set up for a survey with rods spaced at 1-m intervals horizontally (a) and a picture of the field experiment (b).

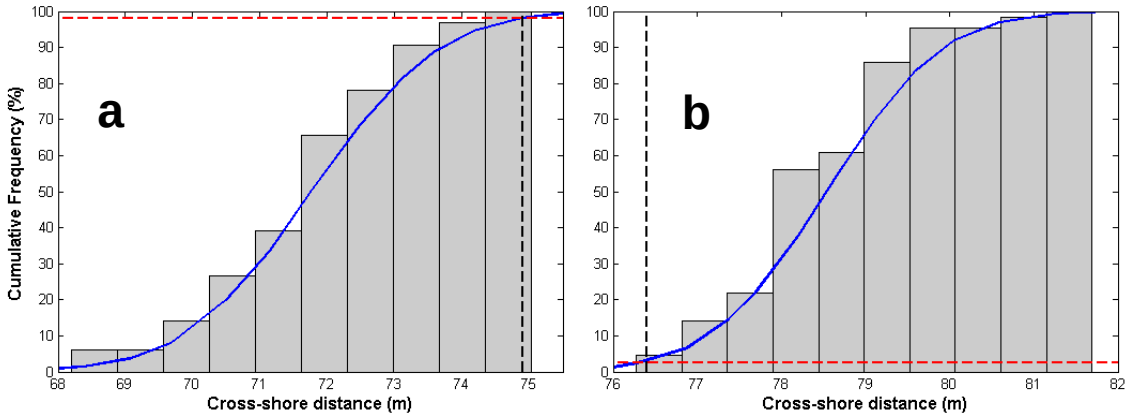

Figure 5. Derivation of 2% exceedance thresholds for run up (a) and run down (b). Bars represent cumulative frequency distribution accompanied by a fitting line (blue). Red dashed line represents the cut off value of interest (98 for run up, 2 for run down) and black dashed line is the corresponding cross-shore location.

Profile topographies were obtained for the transect using Real Time Kinematic Differential Global Positioning System (RTK DGPS), mounted on a staff with a 'flat foot' ensuring surface measurements were recorded. The transect line used was an existing profile currently measured by Plymouth University at monthly intervals, enabling comparison with 6 years' worth of topographic data. Typical accuracies for the RTK DGPS are on the order of 2 cm in both the horizontal and vertical planes. This survey was undertaken prior to any measurements of run up/run down being made.

Video Images

Timex and variance images were collected at the study site every half hour during daylight (e.g. Figure 1). The output images represented the mean (timex) and standard deviation (variance) of image intensity from 600 images sampled at 1 Hz over a 10 minute period. The Argus station at Slapton comprises of three cameras at around 90 m elevation, mounted on a scaffold rig located on cliffs at the north end of the beach, with a collective overview alongshore of around 3 km. Two cameras provide coverage of the survey area, orientated approximately perpendicular to the transect, with images from camera 1 being used for this study. The resolutions afforded by this camera were around 0.2 m cross-shore and 0.5 m alongshore. The data discussed below consists of 35 discrete periods of swash action over four days.

Development of a new methodology

The challenge addressed here is the use of existing time-averaged Argus products to extract R_2 and D_2 without the need for decomposing images into composite frames. In contrast to some previous studies (e.g. Guedes *et al.,* 2011), unrectified (oblique) images were used for this study and standard geometric transformations were applied to the survey transects, allowing transformation between real world (*x, y, z*) and image (*u, v*) coordinate systems (Holland *et al.,* 1997). Unrectified images were used as they were deemed to represent the vertical elevation better after transformation between real world and image coordinates. This solution of geometries takes into account camera parameters and known ground control points, enabling quantitative information to be extracted from the images.

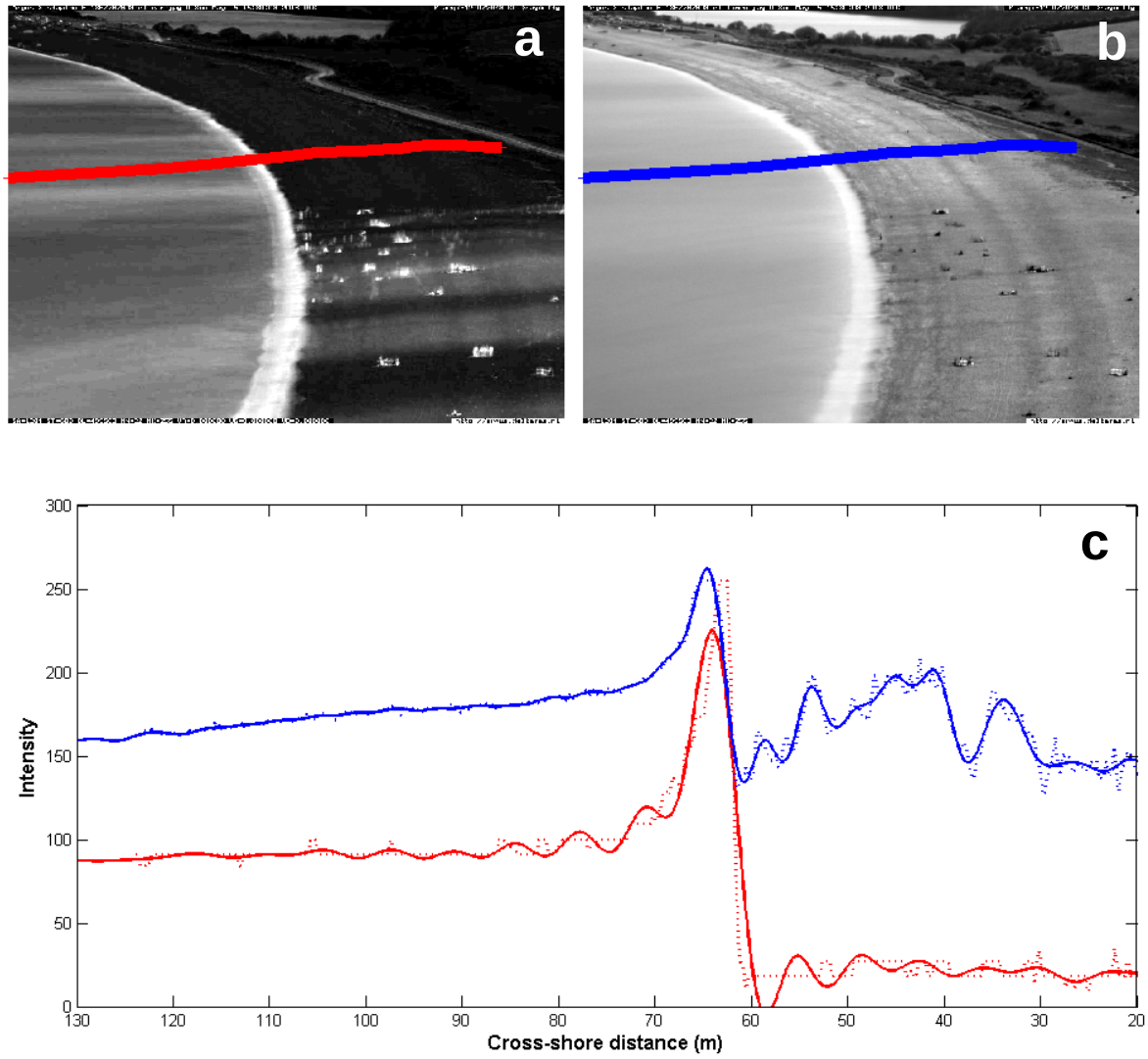

Figure 6. A variance image (a) and corresponding timex image (b) of Slapton Sands taken by camera 1 on 5th May 13. The transect lines have been marked on each image and the corresponding intensity profiles are presented below (c). Variance image intensity is presented as red, with timex presented as blue. Solid lines represent data smoothed by a lowpass filter to attenuate the amplitude of the signal, with dashed lines representing the raw pixel intensities. The x-axis has been flipped so that intensity profile direction matches the orientation of the images. Cross shore distances are taken from nominal benchmarks at the top of the beach.

The dynamic range of intensity in timex and variance images was stretched, increasing the visibility of areas of high intensity in the often dark variance images. Images were then subsequently transformed from RGB images into grayscale for analysis. The RTK DGPS survey co-ordinates were transformed from *x, y* and *z* values into *u* and *v* image co-ordinates, and were then subsequently plotted onto the corresponding images (Figure 6). Profiles were interpolated to 0.1 m increments in the cross-shore direction, with these positions subsequently becoming the sample locations for image intensity. The resulting image intensity profiles were subject to a lowpass filter to attenuate the amplitude of signals. This made subsequent automated analysis possible and intensity

was plotted as a function of cross-shore distance (Figure 6). Once image intensity was plotted for each image, a clear trend emerges, whereby peaks in pixel intensity were generally associated with the shoreline position for both variance and timex images. The subaerial beach was also characterised by comparatively high pixel intensities in the timex images but less so in the variance images.

Having shown the intensity maxima to be co-located with the shoreline, intensity profiles were then normalised against the observations from in-situ field measurments. They were normalised at zero against the R_2 value, this location is referred to as X_R, and normalised at a value of one by the D_2, referred to as X_D. These exceedance thresholds were determined by examination of cumulative frequency distributions of swash for each discrete period of observation. Intensity values were also normalised between the maximum and minimum observed values. The run up and run down events were plotted as separate histograms over the intensity curve to observe and determine the relationship between known parameters (X_R and X_D) and the resulting intensity curve (Figure 7).

The location of the intensity maxima in variance images was seen to be temporally variable, migrating between 0.3 and 0.9 during the sample period, and was thus disregarded as a meaningful method of determining swash parameters. As a result, the lee-side of this intensity maximum was also highly dynamic with negative gradients continuing sometimes to around 1.6 offshore, far below the observed run down limits. Despite the variation observed in the peak and lee slope, the inflection point between low intensities on the subaerial beach and the intensity maxima in the swash zone was remarkably stable, normally co-located at or adjacent to the observed X_R position. The standard deviation of all variance intensity profiles measured was 0.16, reflecting the fact that although the profiles may reflect more or less over the diurnal cycle, the profile shape was consistent throughout with pronounced peaks in the same normalised cross-shore locations. Gradients of the intensity curve in variance images were also highly variable with no obvious persistent peaks or troughs.

Unlike the variance images, the peak in image intensities on the timex images was stable over time, remaining located around 0.6 – 0.7, thus validating its use in previous

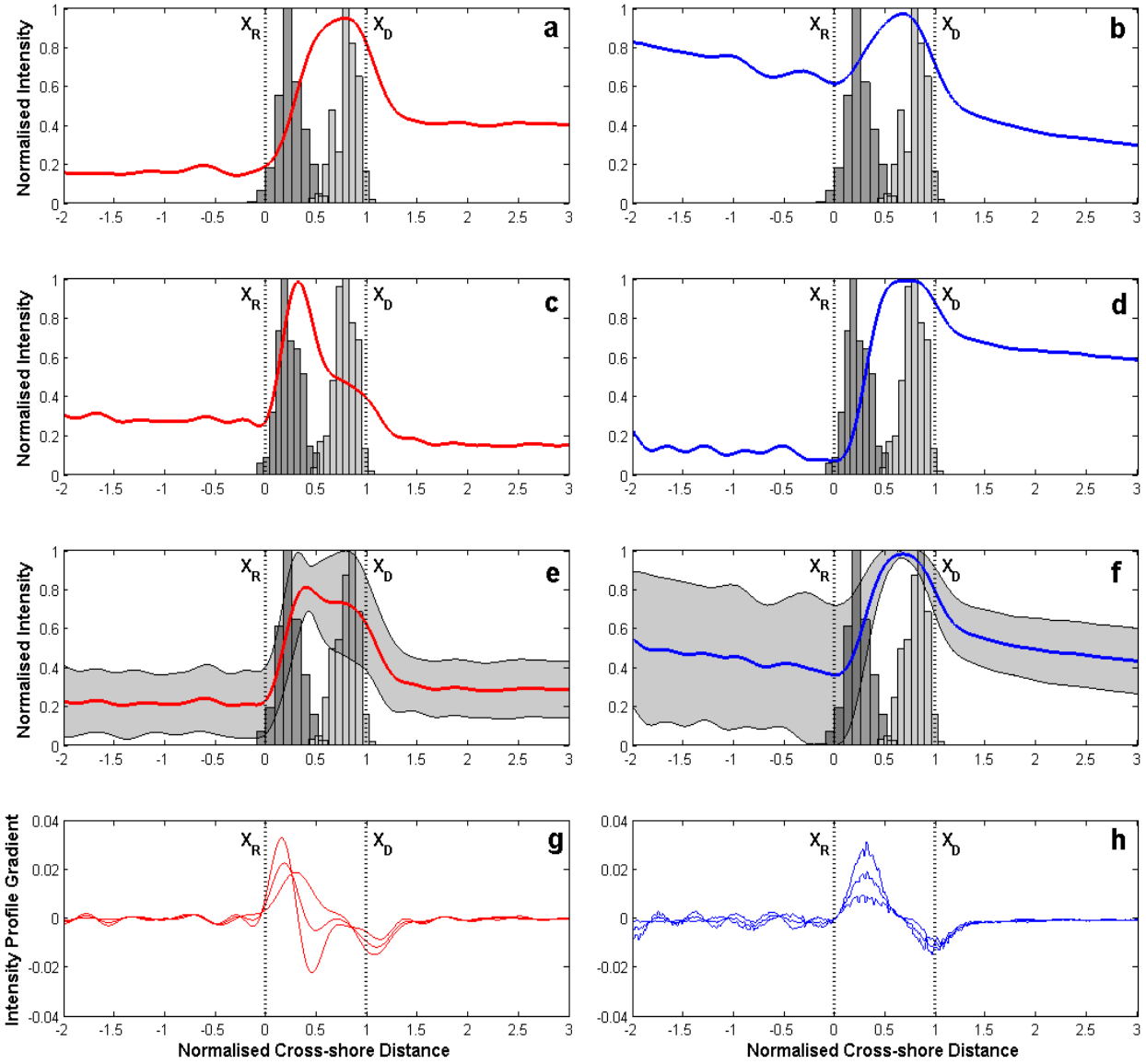

Figure 7. Average image intensity profiles for 21 June (a & b), 24 Jun (c & d) and both days combined (e & f). Variance-derived profiles are presented in the left column with timex-derived profiles on the right. Cross-shore distance has been normalised against X_R (value of zero) and also the X_D (value of one). Histograms represent the distribution of run up (dark grey) and backwash (light grey) for each corresponding period. The standard deviations of image intensity profiles are presented as shaded curves (e & f). Also presented is the gradient of all intensity profiles (g & h).

studies (e.g., Plant and Holman, 1997) as a good indicator of the shoreline position. Plant and Holman's (1997) work has been taken as validation for this method, and no field work was conducted to further validate the predicted still water level. The lee side of this maximum often exhibited negative gradients continuously offshore to the edge of the image. The inflection point between subaerial beach and the intensity maxima was temporally more variable than that observed in the variance, and it was far harder to automatically pick out as a result of high reflectivity of the subaerial beach. Standard deviations of intensity profiles reflect this, with an average value of

0.21 across the whole profile, but 0.36 observed over the subaerial region. Although not observed during this study, analysis of the image archive revealed it was not uncommon for the intensity maxima in the timex images to be located on the subaerial beach during sunny conditions (Figure 8). Despite this, it was still possible to pick out a local intensity maxima that were co-located with the variance intensity maxima and manually evaluate this if required. Analysis of gradients across the intensity profile showed that the peak negative gradient was co-located with X_D during all discrete observations and thus provides a good estimate of run down, and the transition from swash to surf (Figure 7).

As a result of these observations, an automated method was derived to determine X_R, X_D and still water level from images when no field data was available. To determine X_R, the algorithm first looked at the variance images and determined the intensity maxima, before working backwards to the first point at which the gradient of the profile went positive (i.e. the inflection point). The data had to be smoothed for this to work effectively, and as a result, the inflection point was displaced onshore, as demonstrated by the dashed and solid red line in Figure 8. Investigation of this displacement revealed that the true raw inflection point occurred approximately

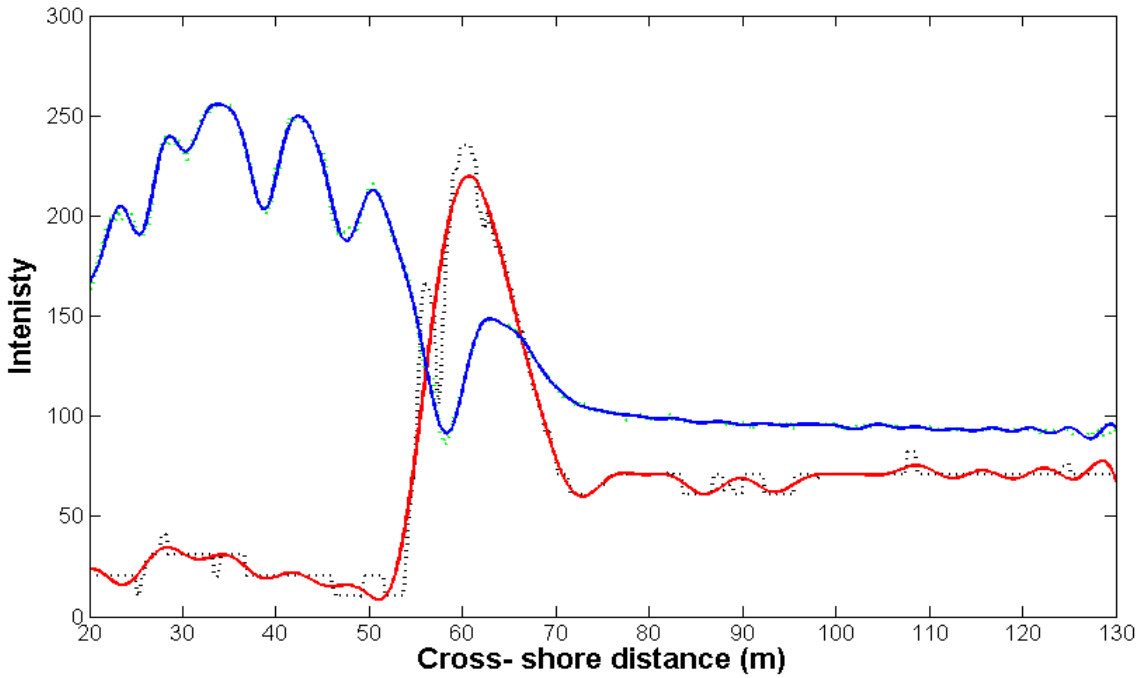

Figure 8. Algorithm derived intensity profiles from variance (red) and timex (blue) images on 3 Feb 09, with unsmoothed data presented as a black dashed line. Of note is the displacement onshore of the inflection point (c. 52 m cross-shore) when converting from raw to smoothed data.

0.17 % along the smoothed curve between inflection and intensity maxima. This was therefore taken to be the position of X_R, and a cross-shore horizontal distance was recorded for this location. In order to ascertain still water level and X_D, an ensemble approach was taken whereby the intensity maxima (still water level) and maximum negative gradient (X_D) in corresponding timex images were used to create the full set of parameters. The cross-shore distances for each of these parameters were then transformed into vertical elevations and recorded as the output. A means of manually checking for error was built into the algorithm, whereby the intensity profiles were shown to the operator and provided they displayed two co-located intensity maxima such as in Figure 6, the operator could assume the outputs were correct. The operator would discard, or manually correct, any results associated with profiles whereby the intensity maxima were not co-located, such as that displayed in Figure 8. This method was able to quantify around 4 images (40 mins of data) in a 1 min period, including time for the operator to quality check the output.

RESULTS

Field Data

The outputs of the algorithm compared well to measured parameters (Figure 9), with strong correlations observed for both run up and backwash. Measured and predicted R_2 values displayed a coefficient of correlation of 0.99, which was significant to 99.9%. Lower run up elevations were seen to be more closely correlated with slightly more

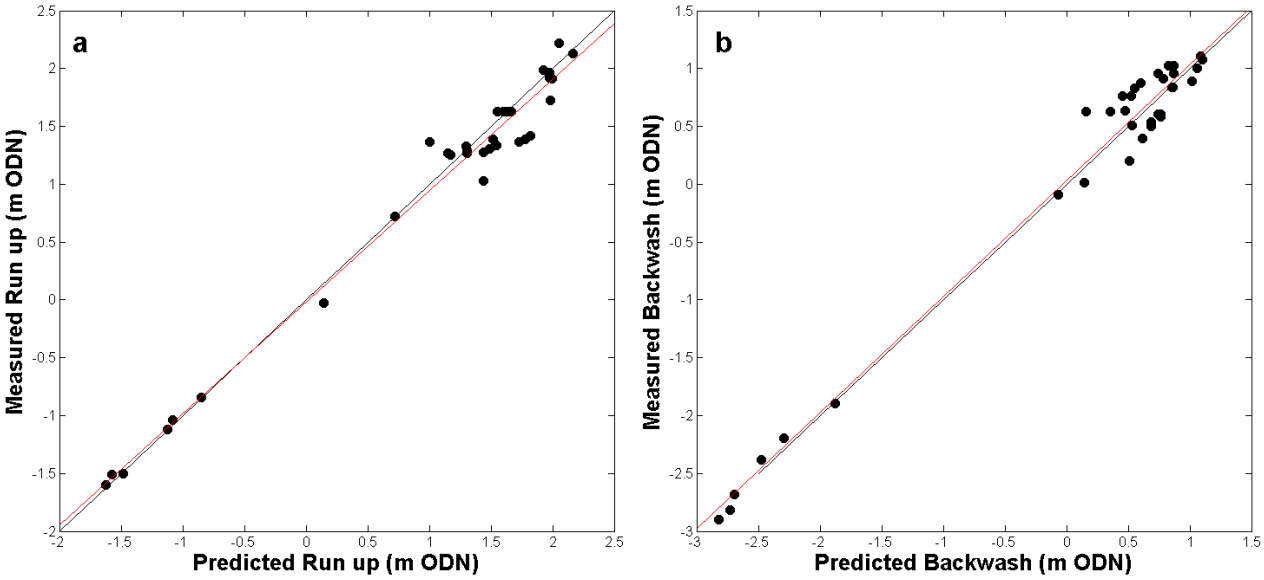

Figure 9. Algorithm derived vertical 2% run up (a) and 2% backwash (b) plotted against measured 2% thresholds. Red line represents linear trend, black line (obscured) represents line of equality.

scatter among events at higher elevations. These are not necessarily higher or more energetic swash events, but merely a function of tidal elevation. The significant wave height does not seem to affect the accuracy of the observed results (Table 1). The standard deviation between measured and observed R_2 was 0.13 m, with a RMS error of 0.17 m. The largest observed vertical error was an under prediction of 0.41 m, with reported values more typically correct to within 0.07 m.

Measured and predicted D_2 values displayed similar trends, with a correlation coefficient of 0.991, significant at 99.9%. The maximum vertical error observed in the D_2 dataset was 0.47 m, with a standard deviation of 0.11 m and a RMS error of 0.18 m.

When considered in the horizontal sense, errors in both R_2 and D_2 were typically less than 1 m (standard deviation = 0.55 m; RMS error = 0.83 m), equating to a pixel error of less 5 pixels. This is potentially a function of the distance of the camera from the survey transect (1.7 km), and would potentially be reduced by a camera in closer proximity.

Application

Having validated this novel method against field data, it was applied to long term datasets consisting of only profile data and Argus imagery. The data was applied to the interim period between survey days, an easterly storm period (H_s 2.3 m) followed by a period of prolonged calm (H_s 0.5 m) during February 2009, an easterly storm (H_s 2.55 m) during April 2008 and an easterly storm (H_s 2.33 m) during March 2008, creating a dataset of 412 individual predictions of R_2, D_2 and still water level (Figure 10). R_2 elevations matched observed changes in morphology well, with the highest values correlated well to the extent of profile changes between pre- and post-event surveys. The run up elevations reported are also, at times, indicative of overtopping of the gravel barrier, which concurs with qualitative analysis of the corresponding Argus images. The dependence of run up on wave height was clear, with predicted run up elevations matching the wave height closely during lower wave conditions but increased scatter at higher wave conditions and around high tide. Still water levels derived from images matched the tidal curve closely but were likely to under-predict the high tide water elevations. These correlations are further explored in Figure 11,

Table 1. Measured and predicted run up and run down values during the study period.

Date	Time (GMT)	H_s (m)	Predicted R_2 (m ODN)	Measured R_2 (m ODN)	Vertical Error (m)	Predicted D_2 (m ODN)	Measured D_2 (m ODN)	Vertical Error (m)
21-Jun	1400	0.73	0.14	-0.03	0.17	-1.88	-1.89	0.02
	1430	0.72	-0.85	-0.85	0.00	-2.29	-2.20	0.10
	1500	0.71	-1.12	-1.12	0.00	-2.69	-2.68	0.01
	1530	0.69	-1.58	-1.51	0.06	-2.82	-2.90	0.08
	1600	0.71	-1.62	-1.60	0.02	-3.04	-2.98	0.06
	1630	0.74	-1.48	-1.50	0.01	-2.73	-2.82	0.09
	1700	0.81	-1.08	-1.03	0.05	-2.47	-2.38	0.09
	1730	0.89	1.00	1.37	0.36	0.53	0.51	0.02
24-Jun	1030	0.59	1.98	1.73	0.25	0.87	0.84	0.03
	1100	0.51	1.98	1.97	0.01	1.06	1.00	0.06
	1130	0.48	2.00	1.91	0.08	1.09	1.10	0.01
	1200	0.44	2.05	2.22	0.17	1.10	1.07	0.03
	1230	0.39	2.17	2.13	0.04	1.02	0.89	0.12
	1300	0.36	1.92	1.99	0.06	0.85	0.84	0.01
	1330	0.36	1.98	1.92	0.06	0.48	0.64	0.16
01-Aug	1100	0.28	1.17	1.26	0.08	0.35	0.63	0.28
	1130	0.27	1.30	1.27	0.04	0.52	0.77	0.24
	1200	0.27	1.44	1.28	0.16	0.60	0.87	0.27
	1230	0.28	1.49	1.30	0.19	0.74	0.96	0.21
	1300	0.31	1.73	1.36	0.36	0.83	1.02	0.19
	1330	0.31	1.78	1.39	0.39	0.87	1.02	0.15
	1400	0.32	1.82	1.42	0.41	0.87	0.96	0.09
	1430	0.33	1.52	1.39	0.13	0.79	0.92	0.13
	1500	0.31	1.54	1.34	0.20	0.55	0.83	0.28
	1530	0.32	1.30	1.29	0.02	0.45	0.77	0.31
02-Aug	1100	0.47	1.15	1.27	0.12	0.16	0.63	0.47
	1130	0.47	0.72	0.72	0.00	-0.07	-0.09	0.03
	1200	0.46	1.44	1.03	0.41	0.14	0.01	0.13
	1230	0.46	1.30	1.33	0.03	0.51	0.20	0.31
	1300	0.45	1.55	1.63	0.08	0.62	0.40	0.22
	1330	0.44	1.60	1.64	0.02	0.69	0.50	0.18
	1400	0.44	1.63	1.63	0.00	0.76	0.61	0.16
	1430	0.42	1.67	1.63	0.04	0.76	0.58	0.18
	1500	0.43	1.67	1.64	0.04	0.74	0.61	0.14
	1530	0.47	1.60	1.62	0.02	0.69	0.54	0.15

where R_2 compared well to the sum of tidal elevation and H_s (R_2 = 0.944), clearly indicating the dominance of the incident wave field in normalising swash action on gravel beaches ($H_s \approx R_2$). Still water levels derived from intensity maxima showed also show a good correlation (0.891) with measured tidal elevations at Devonport.

D_2 values generally look to be accurate throughout the time series presented in Figure 10, however, there is noticeable scatter under energetic wave conditions (H_s > 2 m). Qualitative analysis of the Argus images under these conditions shows that the indicated locations of D_2 are under-predicted, and are typically correlated deep within the surf zone. Of the 412 images analysed, 24 timex images had to be disregarded as a

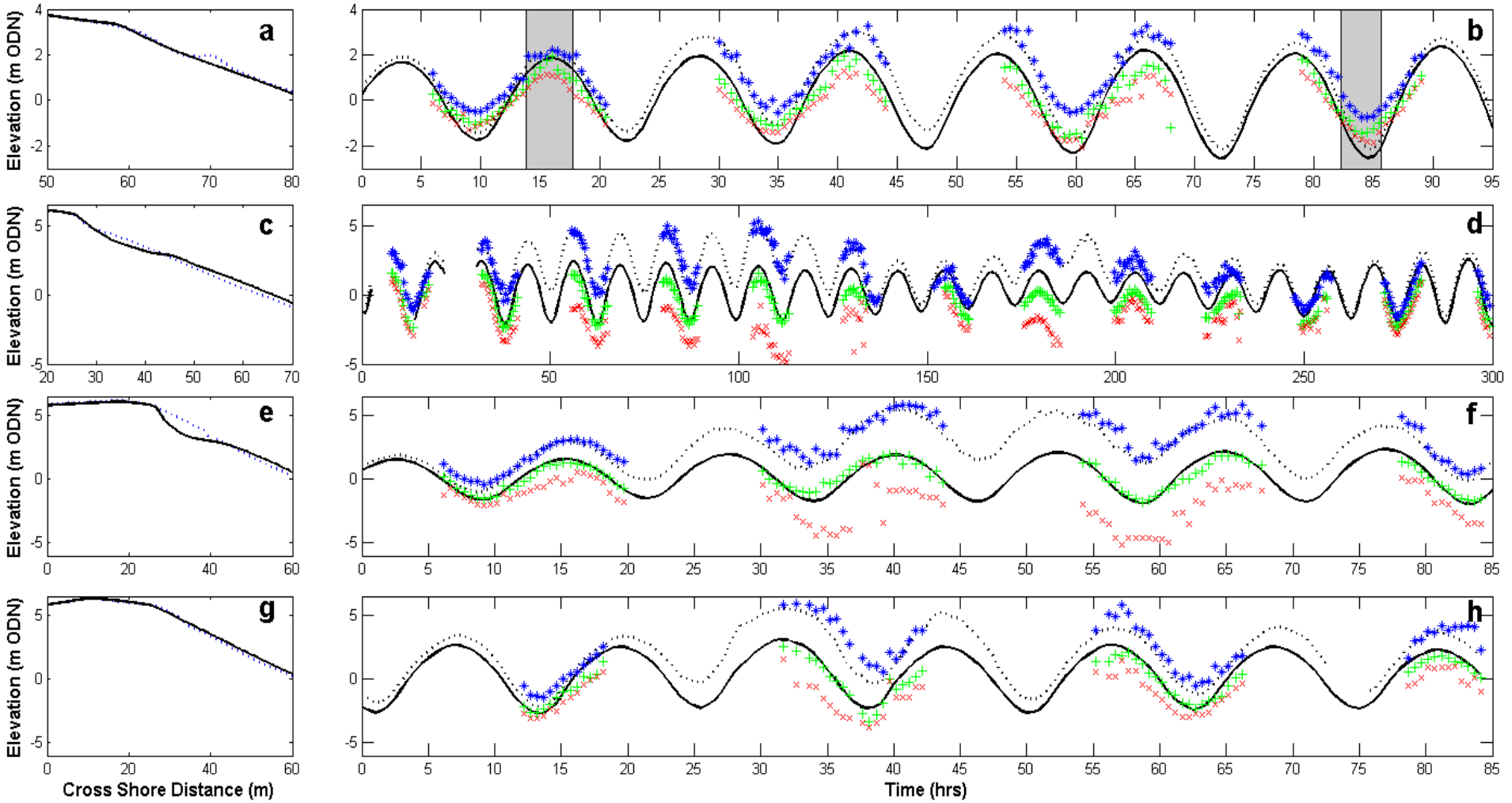

Figure 10. Profile change between 21 – 24 Jun 13 (a) and the accompanying time series (b) of water elevation (black line), Hs (dashed black line) and algorithm derived predictions of 2% run up (blue stars), still water level (green cross) and 2% run down (red crosses). Grey bars indicate the two survey periods, and thus the predictions within have been validated against field measurement. Profile change (c) and time series (d) are also included for storm conditions followed by a prolonged calm period between 28 Jan – 9 Feb 08, easterly storm conditions (e &f) between 16 -19 Apr 08 and southerly storm conditions (g & h) between 9 – 12 Mar 08.

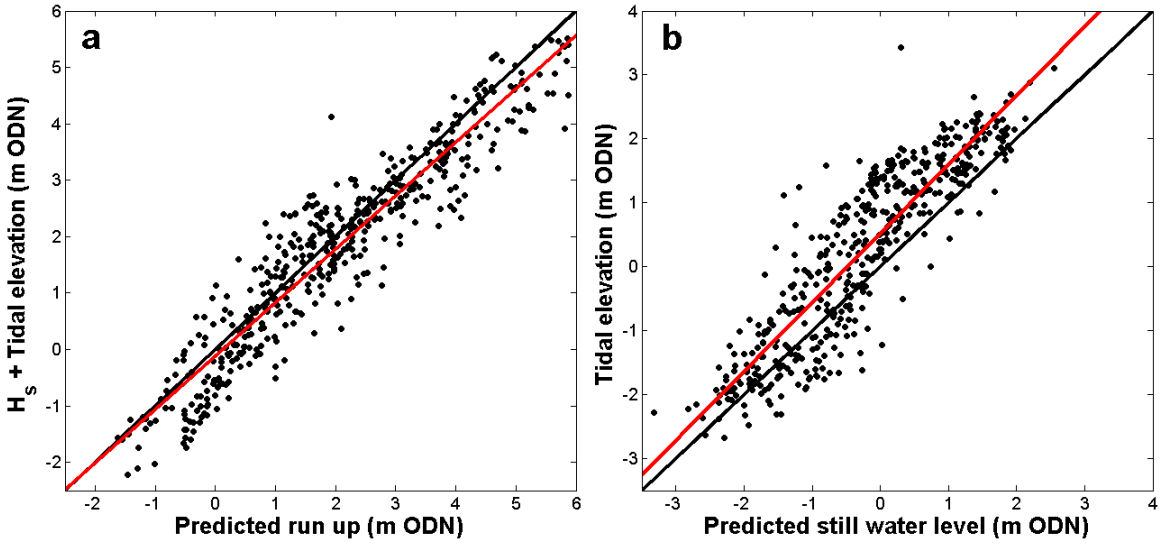

Figure 11. Correlation between algorithm derived R_2 values and the sum of tidal elevation and significant wave height (a) and correlation between algorithm derived still water level and measured tidal elevation at Devonport (b). Black lines represent lines of equality with red lines representing linear fits.

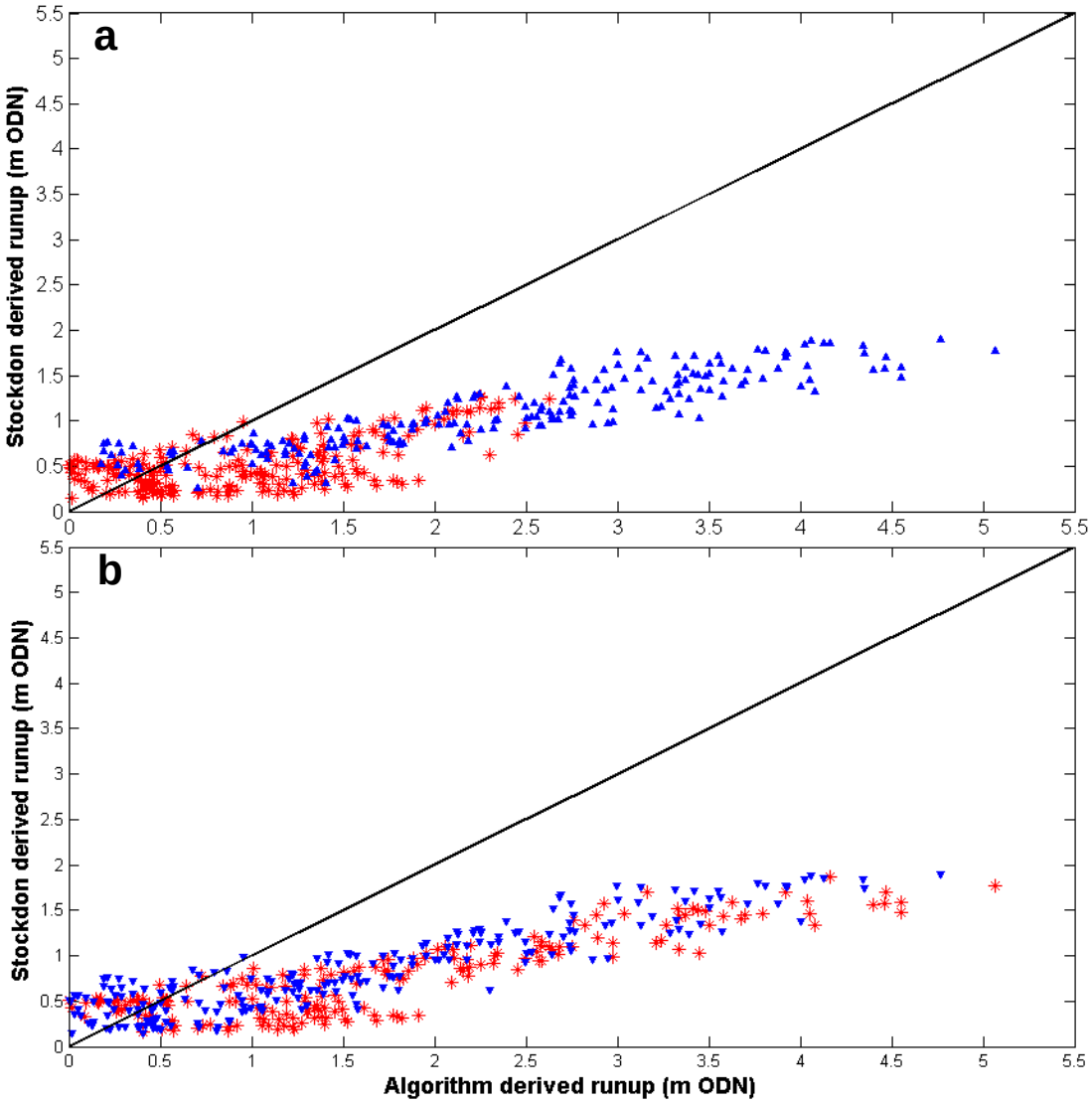

Figure 12. Algorithm derived R_2 run up against R_2 predictions derived from the Stockdon *et al.,* (2006) formula; with black line showing the line of equality. Run up events have been decomposed into wave direction (a), with red stars showing southerly events and blue triangles representing prevailing easterly waves. Furthermore, observations have been decomposed into tidal stage (b) with low tide represented by red stars and high tide represented by blue triangles.

result of quality issues, such as high reflectivity over the beachface or poor weather. The variance images were largely unaffected by the bad weather, with only 1 discarded due to adverse conditions. Typically, however, the variance images still displayed an area of higher variance co-located with the swash zone under foggy and wet conditions, with no discernible effect on the accuracy of the output predictions.

This method has also been compared to Stockdon *et al's.,* (2006) empirical method of predicting R_2 for natural beaches under a range of conditions (hereafter referred to as Stockdon);

$$R_2 = 1.1\left(0.35\,\beta_f(H_oL_o)^{0.5} + \frac{\left[H_oL_o(0.563\beta_f^2 + 0.004)\right]^{0.5}}{2}\right) \quad (2)$$

where β_f denotes foreshore beach slope, H_o denotes deep water wave height and L_o denotes deep water wave length.

Figure 12 shows that on the whole the empirical method is likely to underpredict the R_2 value. Stockdon deals best with conditions dominated by prevailing southerlies at Slapton but still underpredicts a significant number. Swash under more shore-normal easterly conditions is almost entirely underpredicted with only the smallest events being accounted for well. The more energetic conditions are least well predicted, with errors on the order of 2 – 3 m vertically for some easterly swash events. The error on the whole is roughly half the observed run up throughout the dataset, with some scatter at lower values. The tidal stage seems to make little difference to the predictions made by Stockdon, with no discernible difference between low and high tide conditions. Values near zero from the algorithm derived run-up are a result of subtracting the tidal signal from observations, and so in reality this is likely to be a somewhat false value, as there is always likely to be run up, notwithstanding this, the wave conditions in these scenarios are low so the value is not wholly inappropriate.

The method presented here relies on up to date profile information, as indeed do other methods that rely on digitising swash. The sensitivity of the method to profiles was investigated and the results are presented in Figure 13. The storm event from

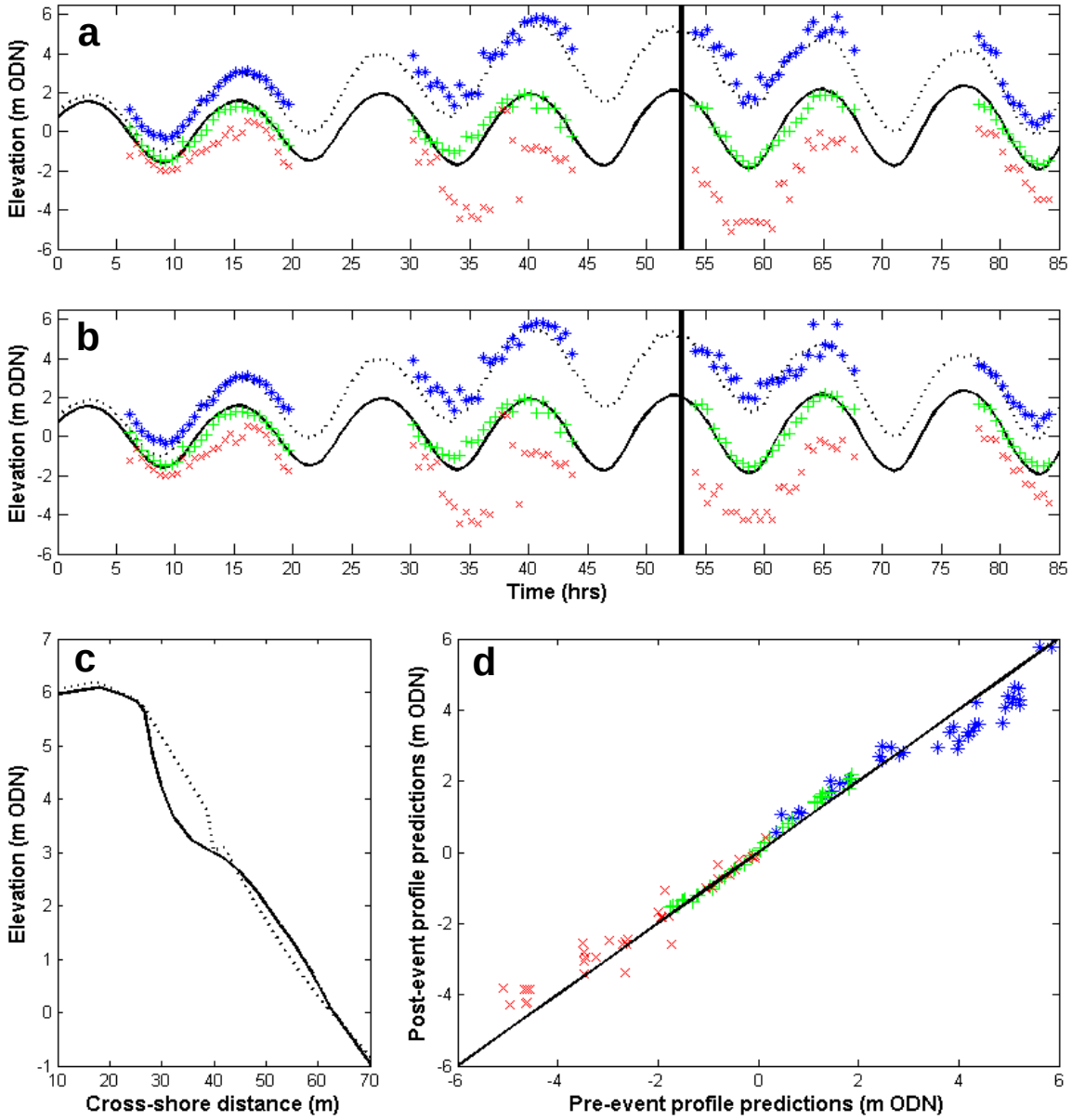

Figure 13. Illustration of the sensitivity of this method to accurate profile data. A storm event between 16-19 Apr 08 is shown in panels a and b, along with predictions of R_2 run up (blue stars), still water level (green crosses) and D_2 run down (red crosses). The pre-event profile has been used throughout in the first time series (a), but the second time series (b) has been fed the post-event profile at 54 hours (solid black line). The pre-event (dashed line) and post-event (solid line) profiles are given (c). The derived parameters from time series a and b are given as a scatter plot (d) with the solid black line indicating the line of equality.

April 2008 presented in Figure 10 was revisited to establish where the biggest swash events took place. It is likely that the highest swash was correlated to the high tide (captured by the images) at 40 hrs or the subsequent high tide around 52 hrs, and an assumption was made that these two events were enough to account for all profile change observed between pre- and post-event profiles. Therefore, from 54 hrs onwards, the algorithm was re-run with the post-event profile data loaded, characterised by high tide erosion and accretion over the mid to low intertidal region.

A correlation of the two outputs is presented in Figure 13 and shows that the output largely matches the profile change, with high tide run up being underpredicted as a result of erosion and mid to low intertidal predictions typically being over estimated as a result of accretion. This arises from the translation of a horizontal optical signature into a vertical position on the profile, and highlights the need for accurate profile information when running this new method, and others that rely on video imaging.

The alongshore variability in morphological change is demonstrated in Figure 14, where the maximum elevation of effective run up is presented; defined here as the maximum height of morphological change between pre- and post-event profiles. This is a useful parameter for a first-order approximation of run up, as it shows the area of the beach that has physically changed as a result of wave action. Stockdon's equation assumes highly accurate wave and profile data is available for each location, when in reality this data is often (as in this case) obtained from a wave buoy in the general area of the study. Again, Stockdon is seen to underpredict on the whole when fed with consistent wave data from one location, with a few anomalously large values as a result of beach profiles. An embayed beach like Slapton Sands experiences all forms of wave transformation, especially refraction over the submerged bathymetry. This easterly storm was mapped reasonably well as the waves propagated past the wave buoy and on towards the beach, whereas under a southerly storm the beach would experience wholly different conditions to those observed by the wave buoy. The algorithm derived values match the general trend in effective run up heights, showing that the method is applicable along-shore without any need for further calibration.

DISCUSSION

This study has provided proof of concept to a new method of remotely sensing swash parameters from video imagery, in fractions of the time reported for methods used hitherto (e.g., Aagard and Holm, 1989; Holman and Guza, 1984). The method needs further extensive field validation, but early indications show that it is of great use in measuring swash parameters. This method uses complete timex and variance images, as opposed to such images decomposed into individual frames. The benefit of this new method is that the speed at which it operates has meant a vast dataset of R_2 and D_2

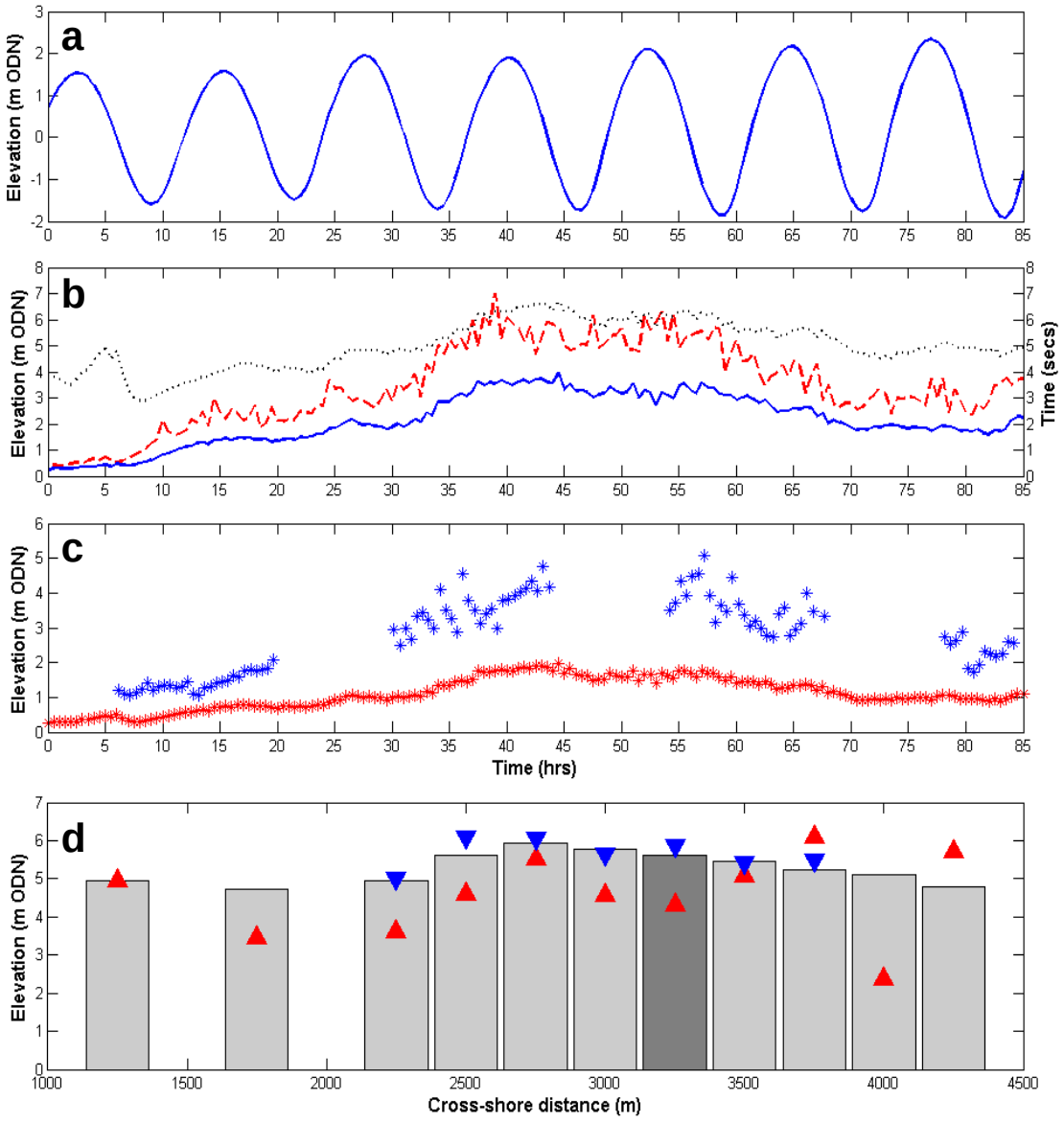

Figure 14. Time series of tidal elevation (a) and wave conditions (b); H_s (blue line), H_m (red dashed line), and T_m (black dashed line) for storm event in April 2008. Stockdon run ups have been solved for the whole event (red stars) along with algorithm derived run ups (blue stars) for hours of daylight and are presented in a raw form without the influence of the tidal elevation (c). Bars (d) show the height of effective run up for profiles along Slapton Sands, defined here as maximum height of morphological change between surveys. The darker shaded bar is the profile that has been used throughout this study. The maximum Stockdon run up (red triangles) has been included (with tidal influence), as has maximum algorithm derived run up for all transects within the field of view of the Argus cameras (blue triangles).

values have been compiled for a range of events, making comparison with existing empirical formulae on a large scale possible.

Variance images are demonstrated to be a more effective means of extracting run up data than timex images, owing to their ability to distinguish between highly reflective (and thus optically intense) areas of subaerial beach against those areas actually

subject to swash action. The reflectivity of subaerial beach as a result of sunlight exposure has previously been seen as a shortfall present with all work relying solely on timex imagery (Quartel, Addink, and Ruessink, 2006). Variance images were seen to show low image intensities across subaerial beach peaking in the swash zone, with the inflection point between these two distinct optical signatures marking the 2% run up exceedance threshold. Errors in this method were comparable to previous studies where manual digitisation of individual swash events has been used; found here to be of the order of 10 cms in the vertical. The method overcomes the problems faced by many researchers investigating the swash zone during high energy events and produced a good estimate of wave run up during storm conditions (Figure 10). Hitherto, Poate *et al.,* (2013) described one of the only methods used to effectively capture high energy events on gravel beaches, in part using temporary cameras recording real-time video at the survey site; this paper presents a method that uses the primary output of existing permanent Argus cameras with no need for real-time video, thus further reducing overall processing time. Although the field validation occurred under predominantly calm conditions, this method provides realistic values for R_2 under extreme storms, even accounting for overtopping. Events on this scale are often not measured in situ due to the likelihood of storm damage to equipment, but with overwash providing a crucial control on barrier migration (Matias *et al.,* 2012), quantitative estimates of such events are important.

The automation of this method has meant that large scale datasets can be compiled and compared in short succession. Stockdon *et al.,* (2006) outlines the importance of understanding the magnitude and longshore variability of extreme run with regard to the prediction of impacts on the hinterland. This new method can be applied to any location in an Argus image for which you have topographic data, providing quantitative data to coastal planners. Although direct measurement of topography is not always possible, it is possible to estimate based on observed tidal translation over time in the images, making assumptions about gradient possible.

In this study, the creation of a measured dataset was compared to the Stockdon *et al.,* (2006) equation for predicting wave run up and found that the predictions consistently underestimated run up on the gravel beach by around half (Figure 12). This concurs

with previous work by Masselink *et al.,* (2013) on gravel beaches in the south of England, where underprediction by Stockdon was found compared to measured run ups derived from digitisation of real time video imagery. This dataset has also been useful in demonstrating how wave run up is often normalised directly by incident wave height on gravel beaches (Figure 11).

Run up has been shown in this study to be linearly dependant on H_s. This is generally well covered in the literature (e.g., Guza and Thornton, 1982), however, much literature incorporates various other parameters such as the surf similarity parameter (Holman and Sallenger, 1985; Ruggiero, Holman, and Beach, 2004; Stockdon *et al.,* 2006) and wave asymmetry (Didenkulova *et al.,* 2013). Prediction of run up on beaches with gentler slopes is more complicated as infragravity motion plays an important part (Ruggiero, Holman, and Beach, 2004; Stockdon *et al.,* 2006), but even so can be scaled using the offshore wave height alone (Senechal *et al.,* 2011). This study shows the assumption that $H_s \approx R_2$ on a steep sloping beach, where infragravity swash is negligible, provides a good first—order approximation of run up. Provided coastal planners know they have a minimum beach slope at a certain site, they can make this assumption based on wave data they have available, without the need to collect profile data too.

The optical signature of back wash was also assessed, and an ensemble approach using timex images provided a good estimate of the 2% exceedance down rush level, based on the maximum negative gradient observed post-peak in intensity profiles. This is a new approach, overcoming the problem of digitising faint downwashes reported in previous studies where manual digitisation of individual frames has been used (e.g., Holman and Sallenger, 1985). This method was not appropriate under storm conditions (H_s > 2 m), where the tail-off from the intensity maxima extended into a wide surf zone, producing observations that were not compatible with what could qualitatively be seen in the images.

The intensity maxima was also investigated as a means of quantifying shoreline location, as has been common practice in previous studies (Plant and Holman, 1997). Despite the use of the variance images in determining run up, the intensity maxima

was temporally very active, shifting between the defined limits of run up and backwash. The timex images showed a much more temporally stable intensity maxima, typically located 60 - 70% of the way between the limits of run up and run down. This confirms previous work in this area that shows the intensity maxima to be a good indicator, however, this work also highlights the dynamic nature of the 'shoreline' and the fact that its quantification could be centered on delimiting the swash zone as a separate zone with relative ease.

CONCLUSIONS

This paper has presented the details and some field validation of a novel remote sensing method for predicting run up and backwash on a gravel beach. The quantification of these parameters is achieved through interrogation of the optical intensity signatures in images collected from a standard coastal imaging system. Run up is quantified using time variance images, where the active swash zone is depicted well as a function of the time-variance (standard deviation) in image intensity. Run down and shoreline is quantified using time lapse images as a function of the time-mean of image intensity. These methods were validated in the field for calm conditions (H_s < 2 m), but extensive subsequent field validation is required. Typically, errors in run up were on the order of 15 cm in the vertical, which is comparable to previous methods utilising manual digitisation of run up. This method is able to compute 2% run up and backwash exceedance distances for a 10 min period in a matter of seconds, and allows the operator the chance to over-ride measurements when intensity profiles are returned that do not conform to the standard form. The use of variance images for quantitative analysis is somewhat novel, where time exposure images are usually favoured; this investigation has indicated that variance images potentially provide more information under adverse field conditions where the quantitative quality of time exposure images is obscured. Field validation shows that this model is well suited to estimation of swash parameters on a gravel beach subject to low wave conditions.

Application of the method to the longer term dataset available at Slapton Sands has shown a consistent under prediction of run up by an existing empirical formula, and highlights the ability of a new, faster method to generate large datasets for continued

validation of empirical methods. This study has also confirmed the direct dependence of swash action on the incident wave field for gravel beaches and the sensitivity of run up estimations to accurate topographic and morphodynamic data.

ACKNOWLEDGEMENTS

The author acknowledges the expert knowledge, guidance and technical assistance provided by Prof. Gerd Masselink and Dr. Mark Davidson throughout the course of this project. Furthermore, the author acknowledges the valuable guidance, input and technical knowledge from Dr. Tim Poate with regard to the Argus station and the georectification of images. Finally, the author acknowledges the on-going work of Plymouth University's Coastal Process Research Group with regard to extensive observation and monitoring at Slapton, making long term comparisons possible.

LITERATURE CITED

Aagaard, T., and Holm, J., 1989. Digitization of wave run-up using video records. *Journal of Coastal Research,* 5(3), 547-551.

Aarninkhof, S.G.J.; Turner, I.L; Dronkers, T.D.T.; Caljouw, M., and Nipius, L., 2003. A video-based technique for mapping intertidal beach bathymetry. *Coastal Engineering,* 49, 275-289.

Almeida, L.P.; Masselink, G.; Russell, P.; Davidson, M.; Poate, T.; McCall, R.; Blenkinsopp, C., and Turner, I., 2013. Observations of the swash zone on a gravel beach during a storm using a laser scanner (Lidar). *Proceedings 12th International Coastal Symposium* (Plymouth, England), *Journal of Coastal Research,* Special Issue No. 65, pp. 636-641.

Austin, M.J., and Masselink, G., 2006. Observations of morphological change and sediment transport on a steep gravel beach. *Marine Geology,* 229, 59-77.

Battjes, J.A., 1974. Surf Similarity. *Proceedings of the 14th Coastal Engineering Conference* (Copenhagen, Denmark, ASCE), pp. 466-480.

Blenkinsopp, C.E.; Turner, I.L.; Masselink, G., and Russell, P.E., 2011. Swash zone sediment fluxes: Field observations. *Coastal Engineering,* 58: 28-44.

Brocchini, M., 2006. Integral swash-zone models. *Continental Shelf Research,* 26: 653-660.

Didenkulova, I.; Denissenko, P.; Rodin, A., and Pelinovsky, E., 2013. Effect of asymmetry of incident wave on the maximum runup height. *Proceedings 12th International Coastal Symposium* (Plymouth, England), *Journal of Coastal Research,* Special Issue No. 65, pp. 207-212.

Erikson, L.; Larson, M., and Hanson, H., 2005. Prediction of swash motion and run-up including the effects of swash interaction. *Coastal Engineering,* 52, 285-302.

Foote, M., and Horn, D., 1999. Video measurement of swash zone hydrodynamics. *Geomorphology,* 29, 59-76.

Guedes, R.M.C.; Calliari, L.J.; Holland, K.T.; Plant, N.G.; Pereira, P.S., and Alves, F.N.A., 2011. Short-term sandbar variability based on video imagery: Comparison between Time-Average and Time-Variance techniques. *Marine Geology,* 289: 122-134.

Guza, R.T., and Thornton, E.B., 1982. Swash oscillations on a natural beach. *Journal of Geophysical Research,* 87(C1), 483-490.

Hails, J.R., 1975. Offshore morphology and sediment distribution, Start Bay. *Philosophical Transactions of the Royal Society of London,* 279, 221-228.

Herbers, T.H.C., and Guza, R.T., 1990. Estimation of directional wave spectra from multicomponent observations. *Journal of Physical Oceanography,* 20, 1703-1724.

Holland, K.T.; Raubenheimer, B.; Guza, R.T., and Holman, R.A., 1995. Run up kinematics on a natural beach. *Journal of Geophysical Research,* 100 (C3), 4985-4993.

Holland, K.T,; Holman, R.A.; Lippmann, T.C.; Stanley, J., and Plant, N.G., 1997. Practical use of video imagery in nearshore oceanographic field studies. *IEEE Journal of Oceanic Engineering,* 22(1), 81-92.

Holman, R.A., 1986. Extreme value statistics for wave run-up on a natural beach. *Coastal Engineering,* 9, 527-544.

Holman, R.A., and Guza, R.T., 1984. Measuring run-up on a natural beach, *Coastal Engineering,* 8, 129-140.

Holman, R.A., and Sallenger, A.H., 1985. Setup and swash on a natural beach. *Journal of Geophysical Research,* 90(C1), 945-953.

Holman, R.A., and Stanley, L., 2007. The history and technical capabilities of Argus. *Coastal Engineering,* 54(6-7), 477-491.

Kingston, K.S.; Ruessink, B.G.; Van Enckevort, I.M.J., and Davidson, M.A., 2000. Artificial neural network correction of remotely sensed sandbar location. *Marine Geology,* 169(1-2), 137-160.

Kobayashi, N., 1997. Wave run up and overtopping on beaches and coastal structures. *Centre for Applied Coastal Research, Delaware; Research Report No. CACR-97-09,* pp. 1-30.

Komar, P.D., 1998. *Beach processes and sedimentation: 2nd edition.* New Jersey: Pearson Education, 544p.

Lippmann, T.C., and Holman, R.A., 1989. Quantification of sand bar morphology: a video technique based on wave dissipation. *Journal of Geophysical Research,* 94(C1), 995-1011.

Lippmann, T.C., and Holman, R.A., 1990. The spatial and temporal variability of sandbar morphology. *Journal of Geophysical Research,* 95(C7), 11575-11590.

Masselink, G., and Puleo, J.A., 2006. Swash-zone morphodynamics. *Continental Shelf Research,* 26, 661-680.

Masselink, G.; Russell, P.; Blenkinsopp, C., and Turner, I., 2010. Swash zone sediment transport, step dynamics and morphological response on a gravel beach. *Marine Geology,* 274, 50-68.

Masselink, G., et al., 2013. Personal Communication.

Matias, A.; Williams, J.J.; Masselink, G., and Ferreira, O., 2012. Overwash threshold for gravel barriers. *Coastal Engineering,* 63, 48-61.

Plant, N.G., and Holman, R.A., 1997. Intertidal beach profile estimation using video images. *Marine Geology,* 140, 1-24.

Plant, N.G., and Holman, R.A., 1998. Extracting morphologic information from field data. *Proceedings of the 26th International Coastal Engineering Conference* (New York, USA, ASCE), pp. 2773-2784.

Poate, T.; Masselink, G.; Davidson, M; McCall, R.; Russell, P., and Turner, I., 2013. High frequency in-situ measurements pf morphological response on a fine gravel beach during energetic wave conditions. *Marine Geology,* 342, 1-13.

Quartel, S.; Addink, E.A., and Ruessink, B.G., 2006. Object-orientated extraction of beach morphology from video images. *International Journal of Applied Earth Observation and Geoinformation,* 8, 256-269.

Ruggiero, P.; Holman, R.A., and Beach, R.A., 2004. Wave run-up on a high-energy dissipative beach. *Journal of Geophysical Research,* 109, C06025, doi: 10.1029/2003JC002160, 2004.

Ruiz de Alegria-Arzaburu, A., and Masselink, G., 2010. Storm response and beach rotation on a gravel beach, Slapton Sands, U.K.. *Marine Geology,* 278, 77-99.

Senechal, N.; Coco, G.; Bryan, K.R., and Holman, R.A., 2011. Wave run up during extreme storm conditions. *Journal of Geophysical Research,* 116, C07032, doi: 10.1029/2010JC006819, 2011.

Stockdon, H.F., and Holman, R.A., 2000. Estimation of wave phase speed and nearshore bathymetry from video imagery. *Journal of Geophysical Research,* 105, 22,015-22,033.

Stockdon, H.F.; Holman, R.A.; Howd, P.A., and Sallenger Jr., A.H., 2006. Empirical parameterization of setup, swash, and run up. *Coastal Engineering,* 53: 573-588.